Preprints of the 21st IFAC World Congress (Virtual)
Berlin, Germany, July 12-17, 2020

Parameter Varying Mode Decoupling for LPV systems

Tamás Baár, Péter Bauer and Tamás Luspay

Institute for Computer Science and Control (SZTAKI), Budapest, Kende u. 13-17., 1111 Hungary (e-mail: baar.tamas@sztaki.hu)

Abstract: The paper presents the design of parameter varying input and output transformations for Linear Parameter Varying systems, which make possible the control of a selected subsystem. In order to achieve the desired decoupling the inputs and outputs of the plant are blended together, and so the MIMO control problem is reduced to a SISO one. The new input of the blended system will only interact with the selected subsystem, while the response of the undesired dynamical part is suppressed in the single output. Decoupling is achieved over the whole parameter range, and no further dynamics are introduced. Linear Matrix Inequality methods form the basis of the proposed approach, where the minimum sensitivity is maximized for the subsystem to be controlled, while the $\mathcal{H}_\infty$ norm of the subsystem to be decoupled is minimized. The method is evaluated on a flexible wing aircraft model.

Keywords: LPV systems, Linear Matrix Inequality, Minimum Sensitivity, Modal Control

1. INTRODUCTION

Since its appearance, Linear Parameter Varying (LPV) systems theory became a well established field in control systems design with numerous application possibilities. Recent trends in systems engineering are pointing in the direction of reducing the complexity of the control problem. This can be achieved by reducing the order of the controller (Nwesaty et al., 2015), by designing fixed structure controllers (Adegas and Stoustrup, 2012), or by decoupling. The paper focuses on the latter one, where our general aim is to control a certain fraction of the system, without affecting other parts.

Various decoupling approaches can be found in the literature for LPV systems to achieve input-output decoupling. (Mohammadpour et al., 2011) designs a static input-output decoupling by pre- and post- compensators based on the singular value decomposition of the steady state transfer function matrix. The method does not introduce further dynamics to the open loop, however it does not guarantee decoupling over the whole frequency range. (Lan et al., 2015) applies a dynamic decoupling based on convex optimalization with Linear Matrix Inequality (LMI) constraints. The $\mathcal{H}_\infty$ norm of a virtual system which is composed by the controlled system and the no coupling reference model is minimized.

In the present paper we focus on subsystem decoupling for LPV systems. In recent years various approaches were introduced in order to assure decoupled control of selected dynamical modes of a system. However to the best of the knowledge of the authors, these methods have not been extended to Linear Parameter Varying (LPV) systems. The common point for many of these methods is that they introduce input and output blending vectors to decouple modes and accordingly reduce the control design into a Single Input Single Output (SISO) problem. (Danowsky et al., 2013) determines an optimal blend for the measurements which assures the isolation of the selected mode, and simultaneously computes an optimal blend for multiple control inputs to suppress the selected mode via a negative optimal feedback, while minimizing the control's effect on other modes. (Pusch, 2018) introduces a joint $\mathcal{H}_2$ norm based input and output blend calculation method which assures the controllability, observability and the independent control of selected modes.

In a recent paper (Baár and Luspay, 2019) the authors presented a novel sensor and actuator blending approach for LTI systems, in order to assure decoupled control of individual modes with simple SISO controllers. The present paper extends these results to LPV systems. Our approach is based on the $\mathcal{H}_-$ index and the $\mathcal{H}_\infty$ norm for LPV systems, by seeking parameter-dependent input and output blend vectors which are maximizing the minimum sensitivity for a given mode, while minimizing the maximal one for the other subsystem. This way decoupling can be achieved between the dynamical modes.

The outline of the paper is as follows. Section 2 describes the problem formulation, followed by Section 3 presenting the necessary mathematical tools. The mode decoupling algorithm is presented in Section 4. Numerical examples are reported in Section 5, followed by the concluding remarks.

2. PROBLEM FORMULATION

2.1 Linear Parameter Varying Systems

Our starting point is the state space formulation of continuous time LPV systems, given as:

$$\mathcal{G}(\rho(t)) : \begin{cases} \dot{x}(t) = A(\rho(t))x(t) + B(\rho(t))u(t), \\ y(t) = C(\rho(t))x(t) + D(\rho(t))u(t), \end{cases} \tag{1}$$

with the standard notation of $x(t) \in \mathbb{R}^{n_x}$, $u(t) \in \mathbb{R}^{n_u}$ and $y(t) \in \mathbb{R}^{n_y}$ being the state, input and output vector, respectively, depending on the continuous time variable t. The trajectories of the time-varying scheduling vector $\rho(t) \in \mathbb{R}^{n_\rho}$ are unknown apriori, but measurable on-line, and they are assumed to be constrained in the parameter variation set

$$\mathcal{F}_\mathcal{P}^\mathcal{V} = \{\rho(t) \in \mathcal{C}^l(R_+, R^{n_\rho}) : \rho(t) \in \mathcal{P},\ \dot{\rho}(t) \in \mathcal{V}, \forall t \geq 0\}, \tag{2}$$

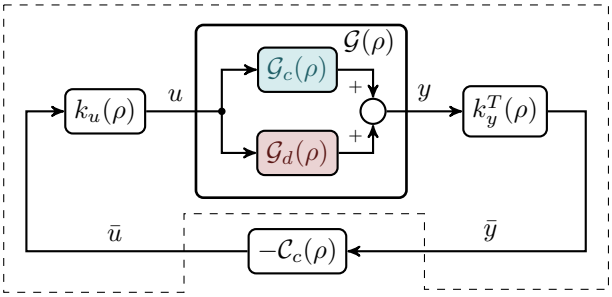

Fig. 1. Proposed closed loop control scheme

where $\mathcal{C}^l$ is the class of piece-wise continuously differentiable functions, $\mathcal{P} := \{\rho \in \mathcal{R}^{n_\rho} : \rho_i \in [\underline{\rho_i}, \bar{\rho_i}]\}$, and $\mathcal{V} := \{\nu \in \mathcal{R}^{n_\rho} : \nu_i \in [\underline{\nu_i}, \bar{\nu_i}]\}$ [1].

We assume that the system matrix functions are given in the following subsystem form:

$$A(\rho) = \begin{bmatrix} A_c(\rho) & 0 \\ 0 & A_d(\rho) \end{bmatrix}, \quad B(\rho) = \begin{bmatrix} B_c(\rho) \\ B_d(\rho) \end{bmatrix}, \\ C(\rho) = [C_c(\rho)\ C_d(\rho)], \quad D(\rho) = [D(\rho)]. \tag{3}$$

For Linear Time Invariant (LTI) systems this form is called the modal form, which can be achieved by a suitable state transformation (Kailath, 1980). A similar structure for LPV systems has been developed, along with the construction of the corresponding parameter-dependent state transformation in (Luspay et al., 2018a), resulting in a block-diagonal and continuous $A(\rho)$ function, where each block represents a dynamical mode of the dynamics. For the ease of presentation, and without loss of generality, assume that the system consists of only two subsystems, one which we would like to control (subscript c) and the one which should be decoupled (subscript d). The latter may contain multiple modes. In (3) coupling between the subsystems appears through the input-output, which we intend to resolve.

Our goal is to create the environment denoted by the dashed frame in Figure 1, which allows the control of the $\mathcal{G}_c(\rho)$ subsystem by a $\mathcal{C}_c(\rho)$ controller, without effecting the other one, $\mathcal{G}_d(\rho)$. This is formalized as maximizing the minimum sensitivity from $\bar{u}$ to $\bar{y}$ through $\mathcal{G}_c(\rho)$ while minimizing the maximum sensitivity through $\mathcal{G}_d(\rho)$. For this purpose we introduce $k_u(\rho) \in \mathbb{R}^{n_u}$ and $k_y(\rho) \in \mathbb{R}^{n_y}$: the normalized (i.e. $\|k_u(\rho)\| = \|k_y(\rho)\| = 1$, $\forall\rho$) input and output blending vector functions, respectively. These blending functions transform the u and y signal vectors onto a single dimension, consequently reducing the control problem into a SISO one. In Figure 1 the control input $\bar{u} \in \mathbb{R}$ is distributed between the plant's inputs ($u = k_u(\rho)\bar{u}$) in a way that they only excite the subsystem which one wishes to control. Similarly the controller's input $\bar{y} = k_y^T(\rho)y \in \mathbb{R}$ is calculated such that the information content from the subsystem which has to be decoupled, is minimized. Formally the blending problem is as follows.

Problem 1. Find normalized $k_u(\rho)$ and $k_y(\rho)$ vector functions such that

$$||k_y^T(\rho)\mathcal{G}_c(\rho)k_u(\rho)||_-^{[\underline{\omega},\bar{\omega}]} > \beta \tag{4}$$

is maximized and

$$||k_y^T(\rho)\mathcal{G}_d(\rho)k_u(\rho)||_\infty < \gamma \tag{5}$$

is minimized over the selected frequency range $[\underline{\omega}, \bar{\omega}]$. Here β and γ are two positive constants referring to the minimal sensitivity and induced $\mathcal{L}_2$ norm, respectively.

[1] Time dependence is omitted in the rest of the paper to ease the notation.

3. MATHEMATICAL BACKGROUND

Basic mathematical definitions are given in the section, which are used throughout the paper.

3.1 Minimum sensitivity

A key notion in the decoupling approach is the minimum sensitivity ($\mathcal{H}_-$ index) of a system, which for LPV systems over a finite frequency range is defined as (Sun et al., 2013):

$$||\mathcal{G}_c(\rho)||_-^{[\underline{\omega},\bar{\omega}]} := \inf_{\omega\in[\underline{\omega},\bar{\omega}]} \underline{\sigma}\left[\mathcal{G}_c(\rho)\right], \ \forall\rho \in \mathcal{F}_\mathcal{P}^\mathcal{V}, \tag{6}$$

with $\underline{\sigma}$ denoting the minimum singular value and $\underline{\omega}$, $\bar{\omega}$ being the minimal and maximal frequency of interest. The computation of (6) can be done based on the Generalized Kalman-Yakubovich-Popov (GKYP) lemma by using convex optimization, involving Linear Matrix Inequality (LMI) constraints. The time-domain interpretation is

$$\inf_{\rho\in\mathcal{F}_\mathcal{P}^\mathcal{V}} \inf_{||u||_2\neq 0} \frac{||y||_2}{||u||_2} > \beta \tag{7}$$

over inputs $u \in \mathcal{L}_2^{n_u}$, such that the following holds:

$$\int_0^\infty \left(\Psi_{11}\dot{x}^T\dot{x} + \Psi_{12}\dot{x}^Tx + \Psi_{21}x^T\dot{x} + \Psi_{22}x^Tx\right) \mathrm{d}t \geq 0 \tag{8}$$

with $x(0) = 0$. Here the matrix Ψ represents the low, middle and high frequency ranges respectively as:

Ω	$\lvert\omega\rvert \leq \bar{\omega}_l$	$\underline{\omega} \leq \omega \leq \bar{\omega}$	$\lvert\omega\rvert \geq \omega_h$
Ψ	$\begin{bmatrix} -1 & 0 \\ 0 & \omega_l^2 \end{bmatrix}$	$\begin{bmatrix} -1 & j\omega_m \\ -j\omega_m & -\underline{\omega}\bar{\omega} \end{bmatrix}$	$\begin{bmatrix} 1 & 0 \\ 0 & -\omega_h^2 \end{bmatrix}$

where $\omega_m = (\underline{\omega} + \bar{\omega})/2$. For further details on the time-domain interpretation see (Iwasaki et al., 2005). The following lemma provides the LMI formulation of the $\mathcal{H}_-$ index for LPV systems, based on (Sun et al., 2013).

Lemma 3.1. Consider the LPV system given by (1). Let $\Pi = \begin{bmatrix} -I & 0 \\ 0 & \beta^2 I \end{bmatrix} \in \mathbb{R}^{(n_x+n_y)\times(n_x+n_y)}$. Assume that (1) is asymptotically stable, and there exists $\beta \geq 0$ and $\Psi \in \mathcal{H}_2$. If there exists $P_c(\rho)$, $Q \in \mathcal{H}_2$ such that $Q \succ 0$ and

$$\begin{bmatrix} A(\rho) & B(\rho) \\ I & 0 \end{bmatrix}^T \begin{bmatrix} \Psi_{11}Q & P_c(\rho) + \Psi_{12}Q \\ P_c(\rho) + \Psi_{21}Q & \dot{P}_c(\rho) + \Psi_{22}Q \end{bmatrix} \begin{bmatrix} A(\rho) & B(\rho) \\ I & 0 \end{bmatrix} \\ + \begin{bmatrix} C(\rho) & D(\rho) \\ 0 & I \end{bmatrix}^T \Pi \begin{bmatrix} C(\rho) & D(\rho) \\ 0 & I \end{bmatrix} \prec 0, \tag{9}$$

holds for all $\rho \in \mathcal{F}_\mathcal{P}^\mathcal{V}$, then $||\mathcal{G}(\rho)||_-^{[\underline{\omega},\bar{\omega}]} \geq \beta$ to a restricted class of input signals specified by (8) with $x(0) = 0$.

In the rest of the paper we will use the middle frequency formulation, and apply the following notation

$$\Xi = \begin{bmatrix} \Psi_{11}Q & P_c(\rho) + \Psi_{12}Q \\ P_c(\rho) + \Psi_{21}Q & \dot{P}_c(\rho) + \Psi_{22}Q \end{bmatrix}. \tag{10}$$

Although stability of the LPV plant is assumed in the derivation of Lemma 3.1, it can be extended and used for unstable systems also. In this case, a stabilizing solution of the parameter-dependent Riccati Inequality is used for computing the minimal sensitivity (see (Liu et al., 2005)).

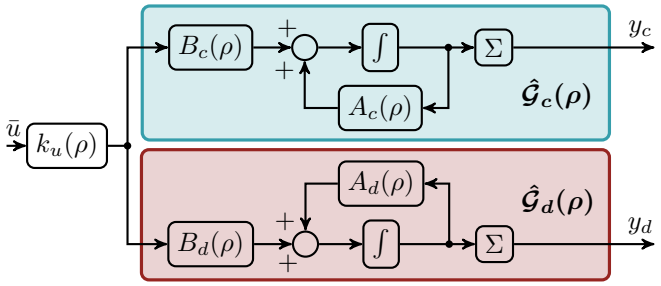

Fig. 2. Input blend calculation

3.2 Maximum sensitivity

The second mathematical tool that we use in the paper is the maximum sensitivity, the induced $\mathcal{L}_2$ norm of LPV systems. The definition reads as:

$$\sup_{\rho\in\mathcal{F}_{\mathcal{P}}^{\mathcal{V}}}\sup_{||u||_2\neq 0}\frac{||y||_2}{||u||_2}<\gamma, \tag{11}$$

which can be efficiently computed using the Bounded Real Lemma for LPV systems (Wu, 1995).

Lemma 3.2. Given the LPV system in (1). If there exists a matrix function $P_d(\rho)\succ 0$ and a positive scalar γ such that (12) is satisfied for all $\rho\in\mathcal{F}_{\mathcal{P}}^{\mathcal{V}}$, then $||\mathcal{G}(\rho)||_2\leq\gamma$ iff

$$\begin{bmatrix} P_d(\rho)A(\rho)+\diamond+C^T(\rho)C(\rho)+\dot{P}_d(\rho) & \star \\ B^T(\rho)P_d(\rho)+D^T(\rho)C(\rho) & D^T(\rho)D(\rho)-\gamma^2 I\end{bmatrix}\prec 0, \tag{12}$$

where $\diamond = A^T(\rho)P_d(\rho)$ and $\star$ is a placeholder for the transpose of the symmetric off-diagonal term. The proof can be found in (Wu, 1995) and is omitted here.

The LMIs (9) and (12) form an infinite number of constraints over the admissible set of the scheduling parameter. Therefore for numerical reasons they are evaluated over a finite grid. More precisely, the parameter variation set is discretized and the corresponding LTI dynamics are obtained. Then, the LMI constraints are written for the finite set of systems, taking into account the bounds of the change in the scheduling parameter. More details can be found in (Wu, 1995).

4. THE PROPOSED DECOUPLING ALGORITHM

The decoupling approach presented in the paper is carried out in two consecutive steps. First an optimal parameter-dependent input blend is found, and applied to the system, next a corresponding output blend function is calculated.

4.1 Input blend calculation

The aim of the subsection is to find an input blend vector function $k_u(\rho)$, which maximizes the excitation of the selected LPV subsystem, while minimizes the impact on the one to be decoupled. In this step only the state dynamics are considered, as it is shown in Figure 2.

Before going into the details side notes has to be taken. It follows from the definition of the $\mathcal{H}_-$ index and the $\mathcal{L}_2$ gain that:

$$||\mathcal{G}_c(\rho)||_{\{-,\infty\}}^{[\omega,\bar{\omega}]}=||\mathcal{G}_c^*(\rho)||_{\{-,\infty\}}^{[\omega,\bar{\omega}]}, \tag{13}$$

where $*$ represents the conjugate system. In other words, the $\mathcal{H}_-$ index and the induced $\mathcal{L}_2$ norm of the system and its conjugate are the same. The use of the conjugate representation assures the linearity in the design process.

At the same time, note that the $\mathcal{H}_-$ index can only be calculated for tall or square systems (Li and Liu, 2010). However, in case the inputs are blended into a scalar $\bar{u}$ signal, then the dual representation would be a wide system. The problem is converted to a square system, by defining the performance output as the sum of the states.

If one writes the LMI constraints of (9) and (12) for the dual system then expresses the formulas in terms of the original representation, one gets (14) and (15), where $\Pi=\begin{bmatrix}-K_u(\rho) & 0\\ 0 & \beta^2 I\end{bmatrix}$. Here we have introduced the new parameter dependent matrix $K_u(\rho)=k_u(\rho)k_u(\rho)^T\in\mathbb{R}^{n_u\times n_u}$, as the dyadic product of the parameter-dependent input blend vectors. Note that the term $D(\rho)=0$.

Note that the $K_u(\rho)$ terms are appearing in the matrix inequalities because of the conjugate representation, otherwise we would be facing a bilinear (and quadratic) matrix problem. The conjugate form ensures linearity, while preserves the corresponding sensitivity values. The newly introduced variable $K_u(\rho)$ has rank 1 for all $\rho\in\mathcal{F}_{\mathcal{P}}^{\mathcal{V}}$, which has to be taken into consideration in the solution. The input blend calculation is summarized in Proposition 4.1.

Proposition 4.1. The optimal $k_u(\rho)$ input blend for the system given in the form of (1) can be calculated as the left parameter dependent singular vector corresponding to the largest singular value of the $K_u(\rho)$ blend matrix, where $K_u(\rho)$ satisfies the following optimization problem

$$\begin{aligned}\underset{P_d(\rho),\,K_u(\rho),\,P_c(\rho),\,Q,\,\beta^2,\,\gamma^2}{\text{minimize}}\quad & -\beta^2+\gamma^2\\ \text{subject to (14), (15),}\quad & 0\preceq K_u(\rho)\preceq I,\ P_d(\rho)\succ 0,\\ & Q\succ 0,\ \text{and rank}\,(K_u(\rho))=1,\ \forall\rho\in\mathcal{F}_{\mathcal{P}}^{\mathcal{V}}\end{aligned} \tag{16}$$

with I being the identity matrix.

Proposition 4.1 is a multi-objective optimization problem, which is frequent in mixed $\mathcal{H}_-/\mathcal{H}_\infty$ fault detection observer design (see e.g. (Wei and Verhaegen, 2008)). Since $K_u(\rho)$ is a parameter dependent matrix, $k_u(\rho)$ can be calculated through an analytic singular value decomposition (Mehrmann and Rath, 1993), which takes into account the parameter dependency and ensures continuity.

The arising rank constraint is satisfied by an alternating projection method. It is taken from (Grigoriadis and Beran, 2000), where the authors applied it for satisfying a coupling rank constraint in a fixed-order $\mathcal{H}_\infty$ control design problem. For the solution of the present problem, the basic idea is the following. Let us denote with Γ_{convex} the convex set which is formed by the LMIs (14) and (15) without the rank constraint on $K_u(\rho)$. Denote this non-convex rank constraint on $K_u(\rho)$ by the set Γ_{rank}. Suppose that the sets have a nonempty intersection, and one wishes to solve the problem by finding a matrix function in the intersection: fulfilling both convex and non-convex constraints. The classical alternating projection scheme states that this problem can be solved by a sequence of orthogonal projections from one set to the other. Each step assures that the projected matrix in the corresponding set has the smallest distance from the one it was projected from. The orthogonal projection theorem also assures that each projection is unique (Luenberger, 1997). However, even if the intersection exists, global

$$\begin{bmatrix} A_c^T(\rho) & C_c^T(\rho) \\ I & 0 \end{bmatrix}^T \Xi \begin{bmatrix} A_c^T(\rho) & C_c^T(\rho) \\ I & 0 \end{bmatrix} + \begin{bmatrix} B_c^T(\rho) & D^T(\rho) \\ 0 & I \end{bmatrix}^T \Pi \begin{bmatrix} B_c^T(\rho) & D^T(\rho) \\ 0 & I \end{bmatrix} \prec 0 \tag{14}$$

$$\begin{bmatrix} P_d(\rho)A_d^T(\rho) + A_d(\rho)P_d(\rho) + B_d(\rho)K_u(\rho)B_d^T(\rho) + \dot{P}(\rho) & P_d(\rho)C_d{}^T(\rho) + B_d(\rho)K_u(\rho)D^T(\rho) \\ C_d(\rho)P_d(\rho) + D(\rho)K_u(\rho)B_d^T(\rho) & D(\rho)K_u(\rho)D^T(\rho) - \gamma^2 I \end{bmatrix} \prec 0 \tag{15}$$

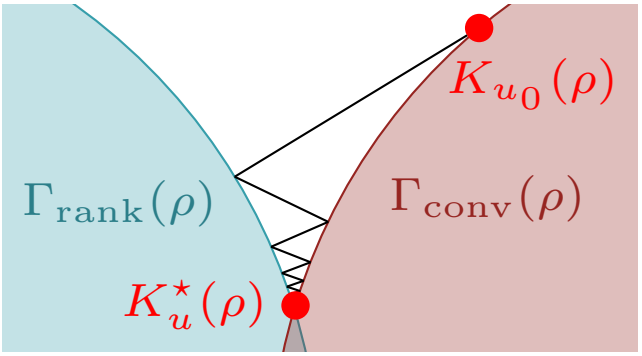

Fig. 3. An alternating projection sequence

convergence cannot be guaranteed in our case, due to the non-convex Γ_{rank} set. Nevertheless local convergence of the proposed algorithm to a matrix which satisfies the above constraints is guaranteed (Grigoriadis and Beran, 2000).

The approach consists of various sequences of alternating projections. In each sequence the rank of the solution is reduced by one (starting from n_u, until $\text{rank}(K_u^\star(\rho)) = 1$ is achieved). The process of a single projection sequence is illustrated in Figure 3. Next, the solution of Proposition 4.1 based on an alternating projection algorithm is presented in details. For this we borrow the following two lemmas from (Grigoriadis and Beran, 2000), and extend them to parameter dependent matrices.

Lemma 4.2. Orthogonal projection to a lower dimensional set. Let $Z(\rho) \in \Gamma_{\text{rank}}^{n\times n}$ and let $Z(\rho) = U(\rho)S(\rho)V^T(\rho)$ be a parameter dependent singular value decomposition of $Z(\rho)$, calculated according to (Mehrmann and Rath, 1993). The orthogonal projection, $Z^\star(\rho) = \text{Proj}_{\Gamma_{\text{rank}}^{n-k}} Z(\rho)$, of $Z(\rho)$ onto the $\Gamma_{\text{rank}}^{n-k\times n-k}$ dimensional set is given by

$$Z^\star(\rho) = U(\rho)S_{n-k}(\rho)V^T(\rho), \tag{17}$$

where the $S_{n-k}(\rho)$ diagonal matrix function is obtained by replacing the smallest k singular value functions by zeros.

Note that the analytic SVD ensures the continuity of the blend vector, in contrast with local solutions. This feature is important from an implementation perspective.

Lemma 4.3. Projection to a general LMI constraint set Γ. Let Γ be a convex set, described by an LMI. Then the projection $X^\star(\rho) = \text{Proj}_\Gamma X(\rho)$ can be computed as the unique solution $Y(\rho)$ to the semidefinite programing problem

$$\begin{aligned} &\text{minimize} \quad \text{trace}(S(\rho)) \\ &\text{subject to} \begin{bmatrix} S(\rho) & Y(\rho) - X(\rho) \\ Y(\rho) - X(\rho) & I \end{bmatrix} \succeq 0, \\ &Y(\rho) \in \Gamma,\ S(\rho), Y(\rho), X(\rho) \in R^{n\times n}, \end{aligned} \tag{18}$$

with $S(\rho) = S^T(\rho)$, $\forall \rho \in \mathcal{F}_{\mathcal{P}}^{\mathcal{V}}$.

4.2 Input blend calculation algorithm

Now we are in the position to present the numerical algorithm to Proposition 4.1. We are using a grid based solution of the problem. LMIs (14), (15) are written as a group of LMIs, with continuously differentiable functions $P_c(\rho)$ and $P_d(\rho)$ evaluated over the finite grid, leading to a finite dimensional convex problem. The following algorithm summarizes the input blend calculation.

Algorithm 1 Input blend calculation

1: The subsystems $\hat{\mathcal{G}}_c$ and $\hat{\mathcal{G}}_d$ are given in the form as shown in Figure 2.
2: A β iteration is carried out in order to find the largest value of β for which the following optimization problem can be solved without rank constraint.

$$\begin{aligned} &\underset{P_d(\rho),\, K_u(\rho),\, P_c(\rho),\, Q,\, \beta^2,\, \gamma^2}{\text{minimize}} \quad -\beta^2 + \gamma^2 + \text{trace}(K_u(\rho)) \\ &\text{subject to (19), (20), } P_d(\rho) \succ 0,\ Q \succ 0, \\ &0 \preceq K_u(\rho) \preceq I,\ \forall \rho \in \mathcal{F}_{\mathcal{P}}^{\mathcal{V}} \end{aligned} \tag{21}$$

Set the counter variable to $k = 1$
3: Alternating projection. Once reached, this point is iterated till convergence is achieved by a suitable selected error metric, such as the relative change in the solution. The previously obtained values of β and γ are kept constant during the iteration, which consists of two steps.
a: Project $K_u(\rho)$ to an $n_u - k$ dimensional subset by Lemma 4.2 to obtain $K_u^\star(\rho)$.
b: Project the achieved reduced rank $K_u^\star(\rho)$ to the LMI constraint set by the following optimization problem

$$\begin{aligned} &\underset{P_d(\rho),\, K_u(\rho),\, P_c(\rho),\, Q,\, S(\rho)}{\min} \quad \text{trace}\,(S(\rho)) \\ &\text{s.t.:(20), (19), } 0 \preceq K_u(\rho) \preceq I,\ Q \succeq 0, \\ &\begin{bmatrix} S(\rho) & K_u(\rho) - K_u^\star(\rho) \\ K_u(\rho) - K_u^\star(\rho) & I \end{bmatrix} \succeq 0 \text{ for } \forall \rho \in \mathcal{F}_{\mathcal{P}}^{\mathcal{V}}. \end{aligned}$$

4: Set $k = k + 1$ and return to step 3, until rank 1 is achieved, then go to step 5.
5: Project $K_u(\rho)$ to an $n_u - k$ dimensional subset by Lemma 4.2. The results is $K_u^\star(\rho)$.
6: Calculate $k_u(\rho)$ as the singular vector corresponding to the largest singular value in the parameter dependent Singular Value Decomposition of $K_u^\star(\rho)$.

Once $k_u(\rho)$ is found, it is applied to the subsystems to give $\bar{A}_{\{c,d\}}(\rho) = A_{\{c,d\}}(\rho)$, $\bar{B}_{\{c,d\}}(\rho) = B_{\{c,d\}}(\rho)k_u(\rho)$, $\bar{C}_{\{c,d\}}(\rho) = C_{\{c,d\}}(\rho)$, $\bar{D}(\rho) = D(\rho)k_u(\rho)$. This notation is used next, to calculate the corresponding output blend.

4.3 Output blend calculation

The output blend will maximize the information of the mode to be controlled to the single output, while it suppresses the effects of the undesired dynamics. The blend calculation process is shown in Figure 4. The direct feedthrough was not involved in the input blend calculation and so it is neglected here. Its effect can be corrected by a $k_y(\rho)^T D(\rho)k_u(\rho)$ feedforward term from $\bar{u}$ to $\bar{y}$ once the output blend is found, by to the following proposition.

Proposition 4.4. The optimal $k_y(\rho)$ output blend for the system shown in Figure 4 can be calculated as the left pa-

$$\begin{bmatrix} P_d(\rho)A_d(\rho) + A_d^T(\rho)P_d(\rho) + C_d^T(\rho)C_d(\rho) + \sum_{i=1}^{n_\rho} \pm \left(v_i \frac{\partial P_d}{\partial \rho_i} \right) & P_d(\rho)B_d(\rho) \\ B_d^T(\rho)P_d(\rho) & -\gamma^2 I \end{bmatrix} \prec 0 \tag{19}$$

$$\begin{bmatrix} A_c(\rho) & B_c(\rho) \\ I & 0 \end{bmatrix}^T \begin{bmatrix} \Psi_{11}Q & P_c(\rho) + \Psi_{12}Q \\ P_c(\rho) + \Psi_{21}Q & \Psi_{22}Q \pm \left(v_i \frac{\partial P_c}{\partial \rho_i} \right) \end{bmatrix} \begin{bmatrix} A_c(\rho) & B_c(\rho) \\ I & 0 \end{bmatrix} + \begin{bmatrix} C_c(\rho) & 0 \\ 0 & I \end{bmatrix}^T \Pi \begin{bmatrix} C_c(\rho) & 0 \\ 0 & I \end{bmatrix} \prec 0 \tag{20}$$

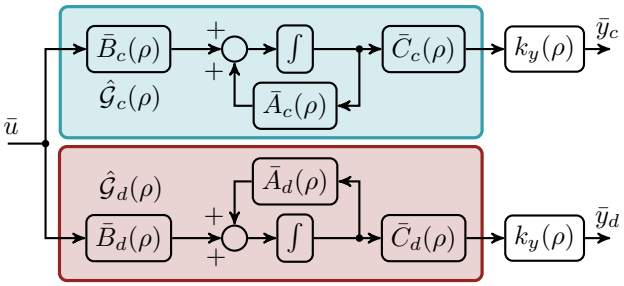

Fig. 4. Problem layout for output blend calculation

rameter dependent singular vector function corresponding to the largest singular value of the $K_y(\rho)$ blend matrix, where $K_y(\rho)$ satisfies the following optimization problem

$$\begin{aligned} &\underset{P_d(\rho),\, K_y(\rho),\, P_c(\rho),\, Q,\, \beta^2,\, \gamma^2}{\text{minimize}} \quad -\beta^2 + \gamma^2 \\ &\text{subject to (23), (24)}, \quad 0 \preceq K_y(\rho) \preceq I,\ P_d(\rho) \succ 0, \\ &Q \succ 0, \text{ and } \operatorname{rank}\left(K_y(\rho)\right) = 1,\ \forall \rho \in \mathcal{F}_{\mathcal{P}}^{\mathcal{V}} \end{aligned} \tag{22}$$

with I being the identity matrix with appropriate dimensions, and $\Pi = \begin{bmatrix} -K_y(\rho) & 0 \\ 0 & \beta^2 I \end{bmatrix}$.

Note that $\bar{D} = 0$ in (23) and (24). The calculation of the output blend vector function can be carried out in a same way as in Algorithm 1, hence it is omitted here.

5. NUMERICAL RESULTS

The presented algorithm was tested on a flexible winged aircraft model, which has been developed in (FLEXOP project, 2015). The aircraft is equipped with eight ailerons (four on the left and four on the right wings) and two ruddervators on each side. Measurements are given at the 90% spanwise location on the left and right trailing edge, providing information about the vertical acceleration (a_z) and the angular rates (ω_x, ω_y) around the lateral and longitudinal axis of the aircraft respectively.

The model has 5 standard aircraft rigid body modes, and two additional flutter modes arising from the coupling of the aerodynamic and structural forces. These flutter modes are responsible for the oscillatory motions of the wing, and they are becoming unstable over a certain airspeed. Further details of the modeling can be found in (Luspay et al., 2018b). An LPV model was created based on the nonlinear one by trimming and linearization, and the indicated airspeed was selected as the scheduling parameter (ρ). The modal form given in (3) was achieved by applying the algorithm of (Luspay et al., 2018a), which was followed by a parameter varying model order reduction. The obtained low order LPV model is used for illustrating the proposed decoupling methodology.

We aim to decouple the rigid body dynamics of the aircraft from the asymmetric flutter mode over the $\rho = [45, 56]$ m/s airspeed range. This would assure that a controller designed for the asymmetric flutter mode, will not interact with the rigid body modes and the corresponding baseline controller. To achieve this, the computation of continuous $k_u(\rho)$ and $k_y(\rho)$ blend vector functions is required. For the parameter-dependent solution a quadratic basis function was selected as $P_{\{c,d\}}(\rho) = P_0 + P_1\rho + P_2\rho^2$. The parameter dependence of the $K_u(\rho)$ and $K_y(\rho)$ blend matrix functions were selected to be linear. The value of $\dot{\rho}$ represents the longitudinal acceleration of the aircraft, and its maximum value was selected to be half of the gravitational acceleration. The LPV theory then assures that the decoupling is achieved when the airspeed is in the designed range, it is changing according to the prescribed basis functions, and $\underline{\dot{\rho}} \leqq \dot{\rho} \leqq \bar{\dot{\rho}}$.

Figure 5 shows the maximal singular values for the subsystems to be controlled and decoupled at various airspeed values. This indicate that there is a certain amount of coupling between the subsystems, because the same input could excite their outputs with a similar magnitude. After solving the blending problem as described in Section 4, the $k_u(\rho)$ and $k_y(\rho)$ blending vector functions were successfully determined and applied to the subsystems. It is possible to evaluate these blending functions at certain airspeed values (frozen parameter): this results in a family of singular value plots corresponding to the decoupled subsystems. This is shown in the lower subfigure. The transfer through the controlled subsystem is also reduced as the blends are suppressing the undesired dynamics.

The transition between grid points is evaluated by time domain simulations. A step input ($\bar{u} = 1(t)$) has been applied to the blended subsystems, while the scheduling parameter has been varying as $\rho(t) = sin(\omega t)$ with ω satisfying conditions on $\dot{\rho}$ used throughout the design. The responses of the two blended subsystems are shown in the lower subfigure of Figure 6. Clearly by the input and output blends, the excitation of the asymmetric flutter mode is higher than the rigid body modes, and so a controller will interact with this mode only. The calculated blending functions are continuous and smooth functions of the parameter, and their evolution is also plotted in Figure 6.

6. SUMMARY

A method for individual control of a selected subsystem was presented for LPV systems. It relies on suitably designed input and output blend vector functions, which are transforming the underlying MIMO plant into a SISO one. The advantage of the method is that, it does not introduce further dynamics into the system. The effectiveness of the method has been validated by a time domain simulation of a flexible wing aircraft. The flexible subsystem was successfully decoupled from the rigid body modes.

ACKNOWLEDGEMENTS

The research leading to these results is part of the FLIPASED project. This project has received funding from

$$\begin{bmatrix} \bar{A}_c(\rho) & \bar{B}_c(\rho) \\ I & 0 \end{bmatrix}^T \Xi \begin{bmatrix} \bar{A}_c(\rho) & \bar{B}_c(\rho) \\ I & 0 \end{bmatrix} + \begin{bmatrix} \bar{C}_c(\rho) & \bar{D}(\rho) \\ 0 & I \end{bmatrix}^T \Pi \begin{bmatrix} \bar{C}_c(\rho) & \bar{D}(\rho) \\ 0 & I \end{bmatrix} \prec 0 \tag{23}$$

$$\begin{bmatrix} P_d(\rho)\bar{A}_d(\rho) + \bar{A}_d^T(\rho)P_d(\rho) + \bar{C}_d^T(\rho)K_y(\rho)\bar{C}_d(\rho) + \dot{P}(\rho) & P_d(\rho)\bar{B}_d(\rho) + \bar{C}_d^T(\rho)K_y(\rho)\bar{D}(\rho) \\ \bar{B}_d^T(\rho)P_d(\rho) + \bar{D}^T(\rho)K_y(\rho)\bar{C}_d(\rho) & \bar{D}^T(\rho)K_y(\rho)\bar{D}(\rho) - \gamma^2 I \end{bmatrix} \prec 0 \tag{24}$$

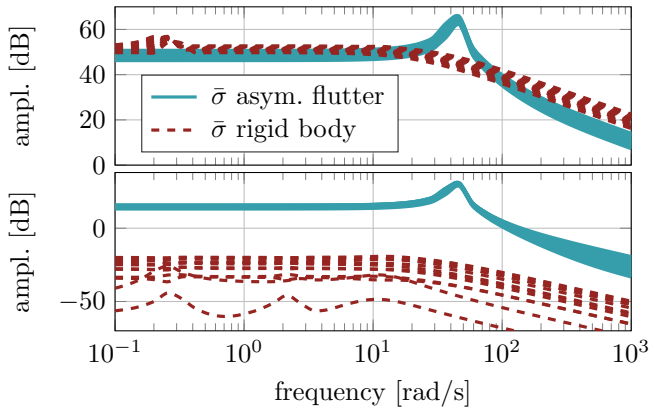

Fig. 5. Frequency domain evaluation of the decoupling example (upper: before blend, lower: after blend)

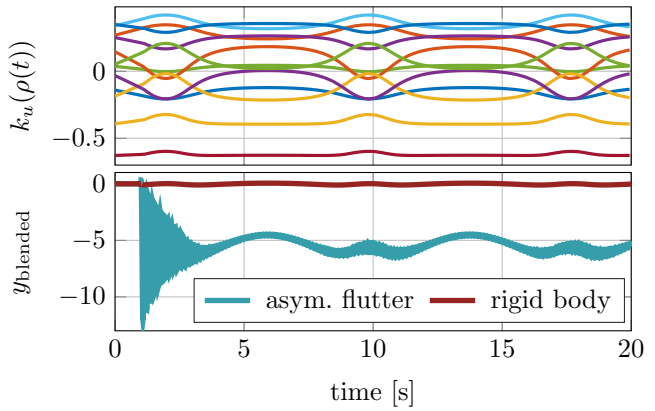

Fig. 6. Time domain evaluation of the decoupling example

the European Unions Horizon 2020 research and innovation programme under grant agreement No 815058. This paper was supported by the Janos Bolyai Research Scholarship of the Hungarian Academy of Sciences. The research reported in this paper was supported by the Higher Education Excellence Program of the Ministry of Human Capacities in the frame of Artificial Intelligence research area of Budapest University of Technology and Economics (BME FIKPMI/FM).

REFERENCES

Adegas, F.D. and Stoustrup, J. (2012). Structured control of LPV systems with application to wind turbines. In *2012 American Control Conference (ACC)*, 756–761. IEEE.

Baár, T. and Luspay, T. (2019). An $H-/H_\infty$ blending for mode decoupling. In *2019 American Control Conference (ACC)*, 175–180. IEEE.

Danowsky, B.P., Thompson, P., Lee, D.C., and Brenner, M.J. (2013). Modal isolation and damping for adaptive aeroservoelastic suppression. In *AIAA Atmospheric Flight Mechanics (AFM) Conference*.

FLEXOP project (2015). Flutter Free FLight Envelope eXpansion for ecOnomical Performance improvement. URL `https://flexop.eu`.

Grigoriadis, K.M. and Beran, E.B. (2000). Alternating projection algorithms for linear matrix inequalities problems with rank constraints. In *Advances in Linear Matrix Inequality Methods in Control*, p. 251–267. SIAM.

Iwasaki, T., Hara, S., and Fradkov, A.L. (2005). Time domain interpretations of frequency domain inequalities on (semi) finite ranges. *Systems & control letters*, 54(7), 681–691.

Kailath, T. (1980). *Linear systems*, volume 156. Prentice-Hall Englewood Cliffs, NJ.

Lan, X., Wang, Y., and Liu, L. (2015). Dynamic decoupling tracking control for the polytopic LPV model of hypersonic vehicle. *Science China Information Sciences*, 58(9), 1–14.

Li, X. and Liu, H.H. (2010). A necessary and sufficient condition for H_- index of linear time-varying systems. In *49th IEEE Conference on Decision and Control (CDC)*, p. 4393–4398. IEEE.

Liu, J., Wang, J.L., and Yang, G.H. (2005). An LMI approach to minimum sensitivity analysis with application to fault detection. *Automatica*, 41(11), p. 1995–2004.

Luenberger, D.G. (1997). *Optimization by vector space methods*. John Wiley & Sons.

Luspay, T., Péni, T., Gőzse, I., Szabó, Z., and Vanek, B. (2018a). Model reduction for LPV systems based on approximate modal decomposition. *International Journal for Numerical Methods in Engineering*, 113(6), p. 891–909.

Luspay, T., Péni, T., and Vanek, B. (2018b). Control oriented reduced order modeling of a flexible winged aircraft. In *2018 IEEE Aerospace Conference*, p. 1–9.

Mehrmann, V. and Rath, W. (1993). Numerical methods for the computation of analytic singular value decompositions. *Electronic Transactions on Numerical Analysis*, 1, 72–88.

Mohammadpour, J., Grigoriadis, K., Franchek, M., Wang, Y.Y., and Haskara, I. (2011). LPV decoupling for control of multivariable systems. *International Journal of Control*, 84(8), 1350–1361.

Nwesaty, W., Bratcu, A.I., and Sename, O. (2015). Reduced-order LPV controller for coordination of power sources within multi-source energy systems. *IFAC-PapersOnLine*, 48(14), 132–137.

Pusch, M. (2018). Aeroelastic mode control using H_2-optimal blends for inputs and outputs. In *2018 AIAA Guidance, Navigation, and Control Conference*.

Sun, G., Ge, D., and Wang, S. (2013). Induced L_2 norm control for LPV system with specified class of disturbance inputs. *Journal of the Franklin Institute*, 350(2), 331–346.

Wei, X. and Verhaegen, M. (2008). Mixed H_-/H_∞ fault detection observer design for LPV systems. In *2008 47th IEEE Conference on Decision and Control*, 1073–1078.

Wu, F. (1995). *Control of Linear Parameter Varying Systems*. University of California, Berkeley.